



ELSEVIER

Earth and Planetary Science Letters 161 (1998) 231–241

EPSL

^{10}Be and ^{26}Al production rates deduced from an instantaneous event within the dendro-calibration curve, the landslide of Köfels, Ötz Valley, Austria

Peter W. Kubik ^{a,*}, Susan Ivy-Ochs ^b, Jozef Masarik ^{c,1}, Martin Frank ^d, Christian Schlüchter ^e

^a Paul Scherrer Institut, c/o Institute of Particle Physics, ETH Hönggerberg, 8093 Zurich, Switzerland

^b Geology Institute, University of Berne, 3012 Berne, Switzerland and Institute of Particle Physics, ETH Hönggerberg, 8093 Zurich, Switzerland

^c Institute of Environmental Physics, EAWAG, 8600 Dübendorf, Switzerland

^d Department of Earth Sciences, University of Oxford, Oxford, OX1 3PR, United Kingdom

^e Geology Institute, University of Berne, 3012 Berne, Switzerland

Received 6 January 1998; revised version received 22 June 1998; accepted 6 July 1998

Abstract

Surface exposure dating requires the knowledge of cosmogenic nuclide production rates. When determining time-integrated production rates the exposure ages of the calibration samples need to be accurately known. The landslide of Köfels (Austria) is very well suited for this purpose. It is the largest landslide in the crystalline Alps of Austria dating back to 7800 ± 100 years BC (AMS ^{14}C dating of buried wood), which is well within the ^{14}C dendro calibration curve. Exposed quartz veins were sampled from the tops of large boulders from the toe of the landslide for analysis of ^{10}Be and ^{26}Al . To calculate sea level, high geomagnetic latitude ($\geq 60^\circ$), open sky radionuclide production rates, corrections were applied for altitude and latitude, for shielding by surrounding mountains, for sample geometry, vegetation and snow cover, and for sample thickness. The production rates for an exposure age of 10,000 years are 5.75 ± 0.24 ^{10}Be atoms/yr g SiO_2 and 37.4 ± 1.9 ^{26}Al atoms/yr g SiO_2 . A $^{26}\text{Al}/^{10}\text{Be}$ ratio of 6.52 ± 0.43 can be calculated. The influence of the geomagnetic field on these production rates has been estimated using two different geomagnetic field records. Our production rates should be a good approximation for the use of surface exposure dating between about 5000 and 13,000 years BP. © 1998 Elsevier Science B.V. All rights reserved.

Keywords: accelerator mass spectrometry; Be-10; Al-26; exposure age; cosmogenic elements

1. Introduction

The measurement of cosmogenic radionuclide concentrations in surface rocks has become a valu-

able tool in dating and characterizing landscape development [1,2]. This method is known as surface exposure dating. It utilizes the buildup of cosmogenic nuclides in specific minerals of a surface rock to determine the time, since the surface has become exposed to the cosmic ray flux.

* Corresponding author. Fax: +41 1 633 1067; E-mail: kubik@particle.phys.ethz.ch

¹ Present address: Department of Nuclear Physics, Komensky University, 842 15 Bratislava, Slovakia.

The measured concentration $N(t)$ of a cosmogenic radionuclide such as ^{10}Be or ^{26}Al can be

expressed as a function of production, radioactive decay, exposure time t , and factors describing the environment of the sampling site.

$$N(t) = P_0 \cdot C \cdot \frac{1 - e^{-\left(\frac{\epsilon \cdot \rho}{\mu} + \lambda\right) \cdot t}}{\frac{\epsilon \cdot \rho}{\mu} + \lambda} + N(0) \cdot e^{-\lambda \cdot t} \quad (1)$$

P_0 is the radioisotope production rate valid for the exposure time and normalized to sea-level, to high geomagnetic latitude ($\geq 60^\circ$) and open sky conditions. C is a product of correction factors which take into account the scaling of P_0 to the altitude and latitude of the sampling location, the shielding of the cosmic ray flux due to the geometry of the landscape and the sample, the burden overlying the actual sample surface such as vegetation, snow, soil, additional rock, and the effective sample thickness. ϵ describes an average erosion rate at the surface for the whole exposure time. ρ is the density of the material being eroded, μ is an effective $1/e$ length for the attenuation of the cosmic ray particles in the rock and the matter above it, and λ is the decay constant of the radionuclide. $N(0)$ is the inherited radionuclide concentration at the beginning of the exposure.

All parameters, except λ and P_0 , are specific to the sampling site and can — in principle — be determined or at least be estimated. As the cosmic ray flux on the surface of the earth changes with time due to changes in the primary galactic cosmic ray flux, due to solar activity and more importantly due to changes in the geomagnetic field, the instantaneous radionuclide production rate is time-dependent. Therefore,

the P_0 , which corresponds to the exposure age of the event investigated by this method, will have to be determined independently.

In the following, only the ^{10}Be ($t_{1/2} = 1.51 \times 10^6$ yr) and ^{26}Al ($t_{1/2} = 7.16 \times 10^5$ yr) production rates in quartz, the most favorable mineral for these radioisotopes, will be discussed. Production rate determinations with the best constrained independent age are listed in Table 1.

The first measurements of ^{10}Be and ^{26}Al time-integrated production rates were made by Nishiizumi et al. [3] in quartz extracted from glacially-polished surfaces in the Sierra Nevada (USA). The exposure time was estimated by constraints on the deglaciation of the area. Using a new estimate of 13,000 yr BP for the glacial retreat [4] and the geographic instead of the geomagnetic latitude of the sampling site as suggested by Ohno and Hamano [5,6] and Sternberg [7,8], Nishiizumi et al. [9] recalculated the ^{10}Be production rate to 5.80. For time scales of millions of years, where the cosmogenic isotope concentrations in the rock surface are assumed to be in saturation, Nishiizumi et al. [10], Brown et al. [11] and Brook et al. [12] obtained production rates in agreement with those of Nishiizumi et al. [3].

Recently, Nishiizumi et al. [9] reported on production of ^{10}Be from water targets exposed to cosmic rays for 1–2 years. Correcting the calculated production rate for quartz (averaged over 4 solar cycles) for the influence of the changes in the geomagnetic field over the last 10,000 years, their new ^{10}Be production rate is in good agreement with the revised original measurement of Nishiizumi et al. [3].

Table 1

Published production rates of ^{10}Be and ^{26}Al (sea-level and geomagnetic latitude $\geq 60^\circ$) and $^{26}\text{Al}/^{10}\text{Be}$ ratios

Method/location	Exposure age	Production rates (atoms/yr g SiO ₂)		$^{26}\text{Al}/^{10}\text{Be}$
		^{10}Be	^{26}Al	
Sierra Nevada rocks [3]	11 kyr	6.03 ± 0.29	36.8 ± 2.7	6.10 ± 0.54
Sierra Nevada rocks [9]	13 kyr	5.80 ^a		
Antarctic rocks [11]	≤2.5 Myr	6.4 ± 1.5 ^b	41.7 ± 5.9 ^b	6.5 ± 1.3
Antarctic rocks [10]	≥4 Myr	6.13		
Antarctic rocks [12]			35 ± 2	
Water target [9]	1–2 yr	6.0 ± 0.3 ^c		
Theoretical [13]	a few Myr	5.97	36.1	6.05

^a Recalculated from Ref. [3] with new estimate of exposure age and use of geographic instead of geomagnetic latitude.

^b Only the smaller of the asymmetric uncertainties quoted in Ref. [11] are listed here.

^c Production rate extrapolated to an exposure time of 10 kyr.

The theoretical calculations of Masarik and Reedy [13] for very long exposure times are in agreement with the ‘measured’ ones. These calculations are based on nuclear systematics, known or estimated cross sections and the development of the cosmic ray cascade through the atmosphere into the rock.

The advantage of measuring production rates which have been time-integrated in the geologic environment is that variations in the galactic cosmic ray flux and changes in the geomagnetic field are already incorporated. In addition, the integration over long time spans smoothes out the effects of these changes making the production rates good approximations for a range of exposure ages close to those of the calibration samples. Because of this integration effect, this range increases when going further back into the past. The disadvantage of this method is that one needs to find samples of an exposure age which has been determined accurately by independent means. The most favorable method for this is radiocarbon dating of an event within the radiocarbon calibration curve, especially if the event would fall within the dendrocalibration curve. We have found such an event in the landslide of Köfels (Austria) which happened about 10,000 years ago.

2. The Köfels event and the sampling locations

9800 years ago a huge landslide occurred above today’s village of Köfels (Ötztal, Tyrol, Austria) which completely blocked the river Ötztaler Ache. During the event, huge rafts of gneiss were released from the Fundus Ridge which must have been at least 250 m higher before the event. They slid across the valley, some remaining intact, others crashed into a rock terrace at the mouth of the Horlachtal valley. Fig. 1 is a simplified map of the area showing the extent of the landslide and the sampling localities.

The volume of material moved was on the order of $2.5 \times 10^9 \text{ m}^3$ making it the largest landslide in the crystalline Alps. The event has received considerable attention [14–16], primarily due to the occurrence of fused rock (pumice of Köfels) at the site. Meteorite impact and a volcanic eruption were initially suggested as possible origins for the scar on the Fundus Ridge above Köfels and the pumice. Ehrismann et al. [17] showed that the energy in a huge landslide

Table 2
 ^{14}C ages

Laboratory	Method	Radiocarbon age
Heidelberg	conventional	$8710 \pm 150^{\text{a}}$
ETH	AMS	$8705 \pm 55^{\text{b}}$
Heidelberg	conventional	$8750 \pm 25^{\text{b}}$

^a Heuberger [19].

^b Ivy-Ochs et al. [18].

would have generated enough heat to melt the gneiss and form the pumice (frictionite). A tunnel drilled through the landslide mass encountered valley fill sediment below the landslide as well as two different pieces of wood from trees which were apparently overrun during the slide. The results of radiocarbon dating these two pieces of wood are listed in Table 2. Details of the radiocarbon dating can be found in Ivy-Ochs et al. [18]. The error-weighted mean radiocarbon age is 8750 ± 25 years. The calibrated age (calendar age) relative to the year 1995 is 9800 ± 100 years [18].

Samples were collected in 1995 and 1996 on both sides of the Ötztal valley. Samples KOE4, 5, 6, 20 were taken from the toe of the landslide at Wolfsegg on the top of Tauferberg east of the river at about 1680 m altitude (see Fig. 1 for sample locations). KOE4, 5, 6 were angular gneiss blocks located within several meters distance to each other. Their size was 1.5–2 m in diameter. The site is dominated by boulders with very little to no fine-grained material. Boulders are wedged against each other on a clast-supported deposit, with large holes between them. One can expect very little fine-grained material even immediately following the event making it a good site for our purpose. Exposed quartz veins (Table 3) were sampled from the flat tops or the edges of the top surface of the boulders which were at least half a meter above ground.

Sample KOE20 was the only boulder measured which had a glacially-polished surface. Glacial polish was inferred based on the presence of irregular sub-parallel scratches, crescentic gouges as well as the gentle rounded shape of the polished surface. The polish occurred on only one side of the block, the other sides had rough surfaces and were only crudely abraded. A quartz vein (Table 3) was chipped off from this polished surface. This boulder was about

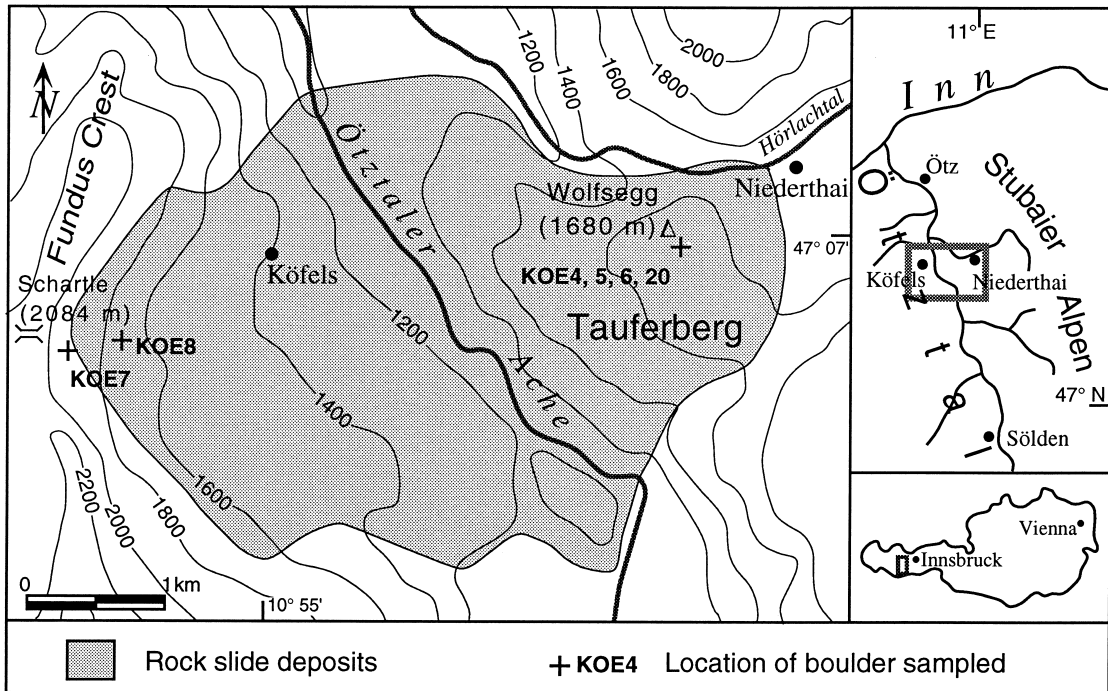


Fig. 1. Map of the Köfels landslide area (modified from Ref. [16]). The sampling locations are labeled KOE4, 5, 6, 20, KOE7 and KOE8. The small maps show the location of the Köfels area with the Ötztal valley and the location of the valley within the borders of Austria.

Table 3

Sample description, mean sample thickness (± 0.5 cm), final weight of quartz and measured ^{10}Be and ^{26}Al concentration

Sample code	Description	Mean sample thickness (cm)	Final weight of quartz (g)	Measured concentration (10^4 atoms/g)	
				^{10}Be	^{26}Al
KOE4	quartz vein	2.75	72.86	21.9 ± 1.3	136.9 ± 11.9
KOE5	quartz vein	4.50	60.29	20.2 ± 1.4	139.5 ± 11.2
KOE6	quartz vein	1.75	75.45	23.3 ± 1.4	146.2 ± 12.9
KOE7	gneiss	1.50	67.94	17.9 ± 1.2	
KOE8	quartz harnish	3.00	45.35	13.2 ± 1.0	121.7 ± 35.8
KOE20	quartz vein	3.50	57.63	19.0 ± 1.2	123.2 ± 9.9

5 m in diameter and 10 m long sitting in the area where the toe of the landslide starts to drop off. One side was sloping steeply to the surrounding ground. On the opposite, uphill side the surrounding ground came closer to the top area (on the order of 20 cm), but was still at least 1 m away from the sampling site.

The surface of Tauferberg is partially overgrown with grass and other vegetation with the big boulders sticking out well from the median surface. Thin pine

trees of about 15 cm diameter and heights of less than 10 m are spread over the sampling area with an average density of less than 10 trees per 100 m^2 .

On the Köfels side of the slide, that is west of the river, 2 locations were sampled. KOE7 is from a boulder field at 1920 m altitude very close to the current crest. The sample came from the flat top of a gneiss boulder (Table 3) which sat on top of several other boulders. There is no indication for the surface to have been covered with soil. The current

density of trees at this location is less than half that at Wolfsegg.

Sample KOE8 (at 1795 m altitude) is from a so-called quartz ‘harnish’. The harnishes found on the slope are thought to be the original sliding surfaces of the landslide. The harnish surfaces were generally flat, and very highly polished, evidencing the heat and friction necessary for their formation. Harnish surfaces were only noted on bedrock outcrops, not on boulders moved during the slide. One of the former was sampled (Table 3) because here one could be sure of no irradiation prior to the landslide. However, this harnish is located in a forested area on the trail up to the mountain crest (Fundus Ridge). Soil was seen on adjacent harnish areas, although KOE8 was in a trail where soil and vegetation had been worn away. The tree cover in this area is currently about 30–35 trees per 100 m² with a diameter of about 20 cm and a height of about 15 m.

3. Sample preparation and analysis

Accelerator mass spectrometry (AMS) was used to determine the isotope ratios ¹⁰Be/Be and ²⁶Al/Al in the Köfels samples. Sample preparation was carried out according to Ivy-Ochs [20]. Before dissolving the final amount of quartz (Table 3), 0.4 to 0.5 mg of the same Be carrier was added, which was used in all our other exposure dating sample preparations [21,22]. No Al carrier was added. The in-situ Al content of the samples was measured in aliquots of the dissolved quartz using ICP AES (inductively coupled plasma atomic emission spectroscopy). For each sample, three standard additions were used in order to avoid matrix effects which could have been different for each sample. The uncertainty of these measurements was less than 1%, based on reproducibility and measurement of solutions of known Al concentration.

The AMS measurements were carried out at the PSI/ETH AMS facility. Each sample was measured at least 3 times together with in-house standard reference materials. Our ¹⁰Be standard (S555) is a secondary standard calibrated to the original material used in the determination of a ¹⁰Be half-life of 1.51 Myr [23], the ²⁶Al standard (ZAL94) is based on the reference material of Sarafin [24]. Both standards

have been employed in our previous exposure dating work, which will allow an easy comparison of all our data. The measured sample isotope ratios were normalized to these standards and then averaged. From this average the ratio of the corresponding chemistry blank was subtracted. This procedure accounts also for any addition of ¹⁰Be contained in the carrier material. The ¹⁰Be/Be ratios of the chemistry blanks were between $1 - 3 \times 10^{-14}$ and correspond on average to a 5% contribution to the measured sample ratios. The chemistry blanks for the ²⁶Al measurements had always ²⁶Al/Al ratios equal to 0 indicating that laboratory contamination is negligible. Sample KOE7 had such a high Al content that the ²⁶Al/Al ratio was below our detection limit.

Measured ¹⁰Be and ²⁶Al concentrations are listed in Table 3. Their uncertainties were determined the following way. First, the uncertainties of the AMS measured isotope ratios of both sample and corresponding standard were added quadratically. Uncertainties associated with the nominal values of the standards are however not included. The uncertainty of a sample average is the larger of either the total statistical error or the 1σ standard deviation of the several measurements. The uncertainty of the corresponding chemistry blank was added quadratically to this. In the case of ²⁶Al, the uncertainties of the stable Al measurements were added in the same manner. Finally, in the calculation of the ¹⁰Be and ²⁶Al concentrations we have added a 5% uncertainty quadratically. This additional uncertainty is the 1σ standard deviation of the ¹⁰Be/Be ratios of several hydrofluoric etching steps after the removal of meteoric ¹⁰Be from quartz grains [20]. The scatter of these ratios should include any variations of the radionuclide concentration in the quartz. It is a very conservative estimate, because it contains also the AMS statistical errors of these measurements.

4. Corrections to production rate calculations

To calculate production rates valid at sea-level and high geomagnetic latitude ($\geq 60^\circ$), the correction factor C in Eq. 1 has to be determined for all our samples. In the following, we discuss and determine corrections for altitude and latitude, for the reduction of the cosmic ray flux by the surrounding moun-

tains and sample geometry, for vegetation, snow, soil burden and the finite sample thickness, for erosion, and for prior exposure. Because of the nonlinear dependence of the correction factors on the various parameters, the calculated uncertainties of these correction factors are not symmetric. We used the larger of the two limits in the calculation of the production rate uncertainties.

4.1. Altitude/latitude correction

For the altitude/latitude correction, the data of table 1 in Lal [1] were interpolated using the geographic instead of the current geomagnetic coordinates of the sampling site (geographic latitude 47.12°N and longitude 10.9°E, Österreichische Karte 25 V (1 : 25,000) Blatt 146, Ötz). For the last 10,000 years, the geomagnetic pole can be roughly approximated by the geographic pole [5–7]. Sternberg [8] estimates that the median difference of the time-integrated, average geomagnetic pole position to the geographic pole is 1.4° for the time range 7–10 kyr. As a conservative estimate for the uncertainty in latitude we have used $\pm 2^\circ$. Altitudes were determined with an altimeter calibrated to reference points on the map (church at Köfels and top of Tauferberg) with an uncertainty of ± 20 m. The measured production rates at the sampling sites have to be scaled down to sea-level and high latitude by a factor of 3.8 for KOE4, 5, 6, 20, by 4.5 for KOE7, and by 4.1 for KOE8. The overall effect of the uncertainties of the input parameters on the altitude/latitude correction is less than 4%. We have, however, not included any uncertainty in the data of table 1 of Lal [1].

4.2. Shielding by mountains and sample geometry

The reduction of the cosmic ray flux due to shielding by the surrounding mountains and due to sample geometry was determined from a 3-dimensional profile of the landscape. Only for sample KOE8 did we need to include a dip of the sample surface (26°). For the angular dependence of the cosmic ray flux intensity $I(\theta)$ we used

$$I(\theta) = I(\theta = 90^\circ) \cdot (\sin(\theta))^m \quad (2)$$

θ = angle to the horizon (dip angle) and $m = 2.3 \pm 1.2$ ([3], and references therein). The integrated

flux for the 4 samples KOE4,5,6,20, which have been used to calculate ^{10}Be and ^{26}Al production rates, is reduced to $99.5 \pm 2.2\%$ of the flux for a completely open sky. The use of $m = 3.5 \pm 1.2$ [25] would have reduced the flux by less than 0.5%. The flux to KOE7 is reduced to $91.3 \pm 8.4\%$ and that for KOE8 to $94.0 \pm 7.7\%$. The maximum uncertainty of the shielding correction factor is due to the uncertainty in m .

4.3. Shielding by vegetation, snow, soil and rock

To estimate the reduction of the production rate by any matter above the sample, an approximation of the real environment was made by stacking mean layers of vegetation, snow and soil on top of the samples. A mean attenuation of the cosmic rays integrated over the effective sample thickness relative to the unshielded 2π surface flux was then calculated taking into account the angular dependence of the flux. The air/surface interface has a strong effect on the cosmic ray neutron flux [13,26,27]. Masarik and Reedy [13] calculated a relatively flat profile for the first 12 g/cm². We assigned a correction factor of 1 to the first 12 ± 1 g/cm². We also used their 157 g/cm² for the 1/e attenuation length of the cosmic ray flux below the surface and assigned a 10% uncertainty to this value. This covers the range of attenuation length values as listed in table 2 of Masarik and Reedy [13].

The thickness of the vegetation layer was approximated by estimating the biomass of the trees found in the sampling areas (mean wood density = 0.8 ± 0.3 g/cm³) and spreading it over the whole area (see Section 2). A long-term snow cover value was estimated from Fliri [28], a compilation of daily snowfall measurements in northern and eastern Tyrol between 1895 and 1991. We selected the 22 stations in valleys, which, like the Ötz Valley, drain northward into the Inn River, and estimated a correlation between mean annual snow cover and altitude. With a 50% uncertainty, we can include all stations into the trend. Four collection sites in the Ötz Valley (data periods: 40–95 years) cover an altitude range between 800 m and 1400 m. The Ötz Valley seems drier than most of the other valleys. We therefore determined its own altitude–snow correlation, from which we calculated a mean annual snow cover of

12.2 cm for KOE4, 5, 6, 20, 14.4 cm for KOE7 and 13.3 cm for KOE8 together with the 50% uncertainty from above. The density of snow was taken as $0.4 \pm 0.2 \text{ g/cm}^2$.

On the one hand, one certainly can argue that the current vegetation cover and a mean annual snow cover deduced from the last 50–100 years cannot describe accurately the environment of the last 10,000 years. On the other hand, one cannot completely ignore cover by vegetation and snow, as the observation periods — even if brief — clearly show. However, even if one did so, the mean production rates calculated for our samples would be only 1.5% less, if we accept the flat profile at the air/surface interface and include the finite sample thickness. It would be 2.5% more, if we ignored vegetation and snow cover and started with exponential attenuation right at the rock surface. We chose to include our estimates for vegetation and snow cover while using the attenuation profile of Masarik and Reedy [13].

Only for sample KOE8 do we definitely have to take soil cover into account. This case will be discussed later on. There is no indication that soil has covered the other samples.

To estimate the uncertainties in the correction factors, we chose a very conservative approach which facilitated the calculations. We decided to calculate worst case scenarios choosing the maximum and minimum values of all parameters involved such that the correction factors became a maximum and minimum for each sample. Shielding by vegetation, snow and the effective sample thickness reduces the cosmic ray flux to $99.3 \pm 3.1\%$ for KOE4, $97.2 \pm 3.0\%$ for KOE5, $100 \pm 2.6\%$ for KOE6, $100 \pm 2.3\%$ for KOE7 and to $98.4 \pm 3.1\%$ for KOE20 relative to the open sky flux. The quoted uncertainties are listed as symmetric errors to facilitate error propagation.

4.4. Erosion

On boulder KOE20 we chipped off glacially-polished quartz veins. There is no indication that more than a few millimeters of the rock could have been eroded away on all our samples qualitatively based on quartz-vein heights. For a 10,000 year event, erosion of this order of magnitude would change the calculated production rates by less than half a per-

cent. Because we actually sampled only the quartz veins, we do not have to worry about erosion at all.

4.5. Prior exposure

Only boulder KOE20 showed glacially polished areas indicating that it came from the original landscape surface. The other boulders sampled (KOE4, 5, 6), which we used to calculate the production rates, do not show these features on any visible surface. This indicates that they came from below the pre-slide surface reducing any effect prior exposure would have had on the measured concentrations. If we had to worry about significant prior exposure, then it would have to be sample KOE20, but this sample actually has the lowest concentration of all 4 calibration samples.

5. Discussion

Table 4 shows ^{10}Be and ^{26}Al production rates valid for sea-level and high latitude calculated using Eq. 1. Based on geological constraints (see below), we selected from the 6 measured samples the 4 samples from Tauferberg to calculate an error-weighted mean for the ^{10}Be and ^{26}Al production rates. The mean, over 9800 years time-integrated production rates are 5.75 ± 0.24 ^{10}Be atoms/yr g quartz and 37.4 ± 1.9 ^{26}Al atoms/yr g quartz. From these values one obtains a $^{26}\text{Al}/^{10}\text{Be}$ ratio of 6.52 ± 0.43 at sea-level and high latitude. The production rates deduced from the Köfels event are in very good agreement with those in Table 1 for the approximately same exposure age.

In the field, we thought that boulder KOE7 may have fallen from the fault scarp at the same time as the rock slide occurred as a whole. The calculated ^{10}Be rate, however, turned out to be so low, that we have to conclude that the boulder fell much later. This is not unreasonable as the very steep scarp remains an active feature with blocks breaking loose periodically. Using the Köfels ^{10}Be production rate, we calculated the exposure age of KOE7 to be 7600 ± 950 years.

The history of KOE8 is quite different from that of KOE7, because the quartz of KOE8 came from a friction-polished surface that is thought to be one

Table 4

¹⁰Be and ²⁶Al production rates for sea-level, high geographic ($\geq 60^\circ$) latitude, open sky and a 10,000 year exposure

Sample code ^a	Production rates (atoms/yr g SiO ₂)		²⁶ Al/ ¹⁰ Be
	¹⁰ Be	²⁶ Al	
KOE4	5.97 ± 0.49	37.7 ± 3.9	6.32±0.83
KOE5	5.62 ± 0.50	39.2 ± 3.8	6.98±0.92
KOE6	6.31 ± 0.51	40.0 ± 4.1	6.33±0.83
KOE20	5.24 ± 0.45	34.2 ± 3.4	6.54±0.85
Weighted mean	5.75 ± 0.24	37.4 ± 1.9	6.52±0.43

^a All samples were collected at an altitude of 1680 m at (geographic) latitude 47.12°N and longitude 10.9°E.

of the original sliding surfaces of the landslide. The very low ¹⁰Be production rate calculated can be explained with soil cover for this sample. A time-averaged soil cover of at least 16 cm can be calculated using the newly determined ¹⁰Be production rate of 5.75 atoms/yr g quartz, the time of the Kőfels event, a soil density of 2.0 ± 0.5 g/cm³, and the uncertainties associated with the measurements, the age and the various correction factors. This value is consistent with observations at the sampling location.

An uncertainty in exposure dating is the assumption of constant radionuclide production rates in the past. Although the forces which both spatially and temporally modulate the cosmic ray flux impinging on the surface of the earth are well known, the magnitude of the variation in the flux with time is not. There are variations in the flux of the primary cosmic rays [29–31], changes in solar activity [32] and variations in the shape and strength of the geomagnetic field [33,34]. Very little is known about the variations of the flux of the galactic cosmic rays on a time scale of only few thousands of years. Changes in solar modulations are also poorly known, except the ones related to the 11-year solar cycle which is of no importance when averaging over 10,000 years. The only factor, though probably the most effective, which is also known to some degree, is the change in the geomagnetic field.

We studied the influence of geomagnetic field intensity on relative, time-integrated ¹⁰Be production rates utilizing two different approaches. The first is based on a combination of the paleomagnetic records of McElhinny and Senanayake [35] for the time period before 8.5 kyr and of Tric et al. [36] for the period 8.6–20 kyr. We have selected these records also because of the much stronger decrease in the

field between 5–6 kyr BP compared to other data sets [37,38]. The influence of this strong excursion should be reflected in the ¹⁰Be production rate profile putting a more stringent lower limit on the time range.

The second approach is based on ¹⁰Be measurements in deep-sea sediments [39]. We first had to convert the ¹⁰Be record into geomagnetic field intensity using new simulation calculations. In this model, the atmospheric ¹⁰Be production rate dependence on the geomagnetic field can be expressed through a polynomial of fifth degree with coefficients dependent on latitude. Similar expressions, fifth degree polynomials with different coefficients, were found also for the production of ¹⁰Be on the earth's surface. Applying these polynomials to our two sets of geomagnetic field intensities, time-dependent production rates of ¹⁰Be were calculated. In both approaches, the instantaneous production rates obtained were integrated with integration steps of 100 years in order to obtain relative, time-integrated production rates for the last 20 kyr. The dependence of calculated production rates on altitude and latitude as a function of geomagnetic field strength was also thoroughly investigated and was found to be negligible. The obtained relation can be taken as universal for all latitudes and for altitudes lower than 10 km. The magnetic field data are shown in Fig. 2 and the results of the production rate simulations in Fig. 3. The calculated production rates in Fig. 3 are normalized to the one determined from the Kőfels event 9800 years ago. The Kőfels rates are 94.1% and 97.6% of today's production rates for the first and for the second approach, respectively.

The uncertainties of the magnetic field data will be reflected in the production rate data. Unfortu-

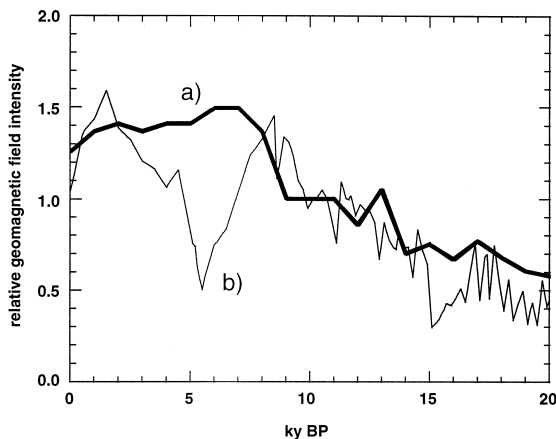


Fig. 2. Relative geomagnetic field intensity as a function of time before present, normalized to the Köfels exposure time. The thick line a) is calculated from the ^{10}Be data of Frank et al. [39]. The thin line b) is a composition of data from McElhinny and Senananyake [35] and Tric et al. [36].

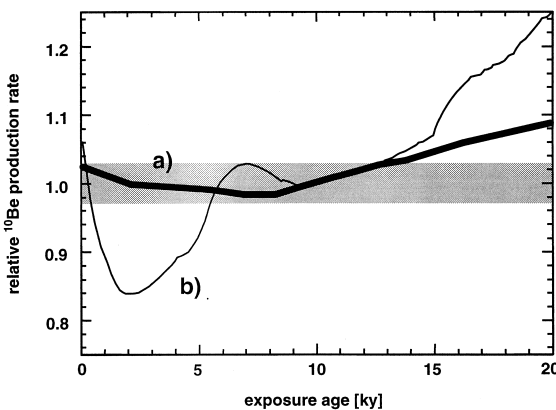


Fig. 3. Time-integrated relative ^{10}Be production rate normalized to the Köfels event as a function of exposure time BP. The thick line a) and the thin line b) correspond to lines a) and b) in Fig. 2, respectively. The shaded area is a band with a width of $\pm 3\%$ relative to the Köfels ^{10}Be production rate.

nately, only uncertainties deduced from the ^{10}Be data of Frank et al. [39] are available to us. Taking these into account, an error band for the relative production rates can be calculated. These errors however are so large (7–10%) that the measured production rate from the Köfels event would be valid for the last 19,000 years. By taking only the mean values of the geomagnetic data as the most probable values, a more conservative estimate of the time range can be

obtained. Let us consider the Köfels ^{10}Be production rate to be a good approximation for the actual ones, if the latter would be within a $\pm 3\%$ band of our new value. Fig. 3 shows that both calculated curves do this for exposure ages between 5500 and 13,000 years. Exposure ages of events in this time range should therefore include an additional uncertainty of 3% when using the cosmogenic radionuclide production rates calibrated at 10 kyr BP. Fig. 3 also indicates that both the Köfels production rates and the other published rates using calibration samples in the same time range, should not necessarily be considered good approximations for exposure dating events on the order of 20,000 years ago. Clearly, more experimental and theoretical work is needed to make the method of exposure dating an absolute dating tool with uncertainties of less than 10%.

6. Conclusions

We have determined ^{10}Be and ^{26}Al production rates for exposure dating by measuring these cosmogenic nuclides in boulders on the surface of the debris which the giant landslide of Köfels (Austria) deposited 9800 years ago. The timing of this event could be measured by radiocarbon dating of pieces of trees buried beneath the debris. This is a rare case, because the time of the landslide lies in the undisputed range of the ^{14}C dendro-chronology. The sea-level and high geomagnetic latitude ($>60^\circ$) production rates for an exposure age of 9800 years are 5.75 ± 0.24 ^{10}Be atoms/yr g quartz and 37.4 ± 1.9 ^{26}Al atoms/yr g quartz. The $^{26}\text{Al}/^{10}\text{Be}$ ratio is 6.52 ± 0.43 . The measured sample concentrations have been corrected for altitude and latitude, for shielding by mountains and sample geometry, for vegetation, snow and finite sample thickness. Other possible corrections such as erosion or prior exposure have been investigated.

Calculations have been performed to estimate the influence of the geomagnetic field over the last 20,000 years on the new production rates. Our calculations show that for the time between about 5500 yr BP and 13,000 yr BP the actual production rates should lie within $\pm 3\%$ of the one determined from the Köfels event. Conversely, going further back in time the production rates determined here may no

longer be as good an approximation as they are for the period between 5.5 and 13 ka. More experimental and theoretical work is needed to make exposure dating a method with absolute uncertainties of less than 10%.

Acknowledgements

The authors would like to thank H. Kerschner and R. Sailer for their help during the field trips, and the AMS accelerator crew P. Kägi, R. Gruber and J. Thut for making sure that everything was ready and running on time. *[MK]*

References

- [1] D. Lal, Cosmic ray labeling of erosion surfaces: in situ nuclide production rates and erosion models, *Earth Planet. Sci. Lett.* 104 (1991) 424–439.
- [2] T. Cerling, H. Craig, Geomorphology and in-situ cosmogenic isotopes, *Annu. Rev. Earth Planet. Sci.* 22 (1994) 273–317.
- [3] K. Nishiizumi, E.L. Winterer, C.P. Kohl, J. Klein, R. Middleton, D. Lal, J.R. Arnold, Cosmic ray production rates of ^{10}Be and ^{26}Al in quartz from glacially polished rocks, *J. Geophys. Res.* 94 (12) (1989) 17907–17915.
- [4] D.H. Clark, P.R. Bierman, P. Larsen, Improving in situ cosmogenic chronometers, *Quat. Res.* 44 (1995) 367–377.
- [5] M. Ohno, Y. Hamano, Geomagnetic poles over the past 10,000 years, *Geophys. Res. Lett.* 19 (1992) 1715–1718.
- [6] M. Ohno, Y. Hamano, Global analysis of the geomagnetic field: time variation of the dipole moment and the geomagnetic pole in the Holocene, *J. Geomagn. Geoelectr.* 45 (1993) 1455–1466.
- [7] R.S. Sternberg, Radiocarbon fluctuations and the geomagnetic field, in: R.E. Taylor et al. (Eds.), *Radiocarbon After Four Decades*, Springer, New York, 1992, pp. 93–116.
- [8] R. Sternberg, Paleomagnetic averages of geomagnetic latitude, *Radiocarbon* 38 (1) (1996) 169–170.
- [9] K. Nishiizumi, R.C. Finkel, J. Klein, C.P. Kohl, Cosmogenic production of ^7Be and ^{10}Be in water targets, *J. Geophys. Res.* 101 (B10) (1996) 22225–22232.
- [10] K. Nishiizumi, C.P. Kohl, J.R. Arnold, J. Klein, D. Fink, R. Middleton, Cosmic ray produced ^{10}Be and ^{26}Al in Antarctic rocks: exposure and erosion history, *Earth Planet. Sci. Lett.* 104 (1991) 440–454.
- [11] E.T. Brown, J.M. Edmond, G.M. Raisbeck, F. Yiou, M.D. Kurz, E.J. Brook, Examination of surface exposure ages in Antarctic moraines using in situ produced ^{10}Be and ^{26}Al , *Geochim. Cosmochim. Acta* 55 (1991) 2269–2283.
- [12] E.J. Brook, E.T. Brown, M.D. Kurz, G. Raisbeck, F. Yiou, An Antarctic perspective on in-situ cosmogenic nuclide production, *Radiocarbon* 38 (1) (1996) 150.
- [13] J. Masarik, R.C. Reedy, Terrestrial cosmogenic-nuclide production systematics calculated from numerical simulations, *Earth Planet. Sci. Lett.* 136 (1995) 381–395.
- [14] G. Abele, Bergstürze in den Alpen, ihre Verbreitung, Morphologie und Folgeerscheinungen, *Alpenvereinshefte* 25, München, 1974.
- [15] E. Preuss, Gleitflächen und neue Friktionitfunde im Bergsturz von Köfels im Ötztal, Tirol, *Mater. Technik* 14 (1986) 169–174.
- [16] H. Heuberger, The giant rockslide of Köfels, Ötztal, Tyrol, *Mt. Res. Dev.* 14 (H4) (1994) 290–294.
- [17] T.H. Erismann, H. Heuberger, E. Preuss, Der Bimstein von Köfels (Tirol), ein Bergsturz-‘Friktionit’, *Tschermaks Mineral. Petrogr. Mitt.* 24 (1977) 67–119.
- [18] S. Ivy-Ochs, H. Heuberger, P.W. Kubik, H. Kerschner, G. Bonani, M. Frank, C. Schlüchter, The age of the Köfels event - relative, ^{14}C and cosmogenic isotope dating of an early Holocene landslide in the Central Alps (Tyrol, Austria), *Z. Gletscherkd. Glazialgeol.* 34 (1998) 57–68.
- [19] H. Heuberger, Gletschergeschichtliche Untersuchungen in den Zentralalpen zwischen Sellrain- und Ötztal, *Wissenschaftliche Alpenvereinshefte* 20, Universitätsverlag Wagner, Innsbruck, Austria, 1966.
- [20] S. Ivy-Ochs, The dating of rock surfaces using in situ produced ^{10}Be , ^{26}Al and ^{36}Cl , with examples from Antarctica and the Swiss Alps, Ph.D. dissertation no. 11763, ETH Zurich, Switzerland, 1996.
- [21] S. Ivy-Ochs, C. Schlüchter, P.W. Kubik, B. Dittrich-Hannen, J. Beer, Minimum ^{10}Be exposure ages of Early Pliocene for the Table Mountain plateau and the Sirius Group at Mount Fleming, Dry Valleys, Antarctica, *Geology* 23 (1995) 1007–1010.
- [22] S. Ivy-Ochs, C. Schlüchter, P.W. Kubik, H.-A. Synal, J. Beer, H. Kerschner, The exposure ages of an Egesen moraine at Julier Pass, Switzerland, measured with the cosmogenic radionuclides ^{10}Be , ^{26}Al and ^{36}Cl , *Eclogae Geol. Helv.* 89 (1996) 1049–1063.
- [23] H.J. Hofmann, J. Beer, G. Bonani, H.R. von Gunten, S. Raman, M. Suter, R.L. Walker, W. Wölfl, D. Zimmermann, ^{10}Be : Half-life and AMS-standards, *Nucl. Instr. Meth. B* 29 (1987) 32–36.
- [24] R. Sarafin, Anwendung radiochemischer Methoden und der Beschleuniger-Massenspektrometrie zur Bestimmung der tiefenabhängigen, langlebigen Spallations-Radionuklide ^{10}Be , ^{26}Al , ^{36}Cl and ^{53}Mn in Steinmeteoriten und Gedanken zum ungeklärten Ursprung der Shergottite, Ph.D. dissertation, Universität zu Köln, Germany, 1985.
- [25] E. Heidebreder, K. Pinkau, C. Reppin, V. Schönfelder, Measurements of the distribution in energy and angle of high-energy neutrons in the lower atmosphere, *J. Geophys. Res.* 76 (1971) 2905–2916.
- [26] K. O’Brien, H.A. Sandmeier, G.E. Hansen, J.E. Campbell, Cosmic ray induced neutron background sources and fluxes for geometries of air over water, ground, iron and aluminum, *J. Geophys. Res.* 83 (1978) 114–120.

- [27] L. Dep, D. Elmore, J. Fabryka-Martin, J. Masarik, R.C. Reedy, Production rate systematics of in-situ produced cosmogenic nuclides in terrestrial rocks: Monte Carlo approach of investigating $^{35}\text{Cl}(n, \gamma)^{36}\text{Cl}$, *Nucl. Instr. Meth. B92* (1994) 321–325.
- [28] F. Fliri, *Der Schnee in Nord- und Osttirol 1895-1991, Ein Graphik-Atlas mit 163 Tabellen*, vol. 2, Universitätsverlag Wagner, Innsbruck, Austria, 1992.
- [29] D. Fink, J. Klein, R. Middleton, S. Vogt, G.F. Herzog, ^{41}Ca in iron falls, Grant and Estherville: production rates and related exposure age calculations, *Earth Planet. Sci. Lett.* 107 (1990) 115–128.
- [30] J. Klein, D. Fink, R. Middleton, S. Vogt, G.F. Herzog, R.C. Reedy, J.M. Sisterson, A.M. Koehler, A. Magliss, Average SCR flux during the past 10^5 years: Inference from ^{41}Ca in lunar rock 74275, XXI Lunar and Planet. Sci. Conf., Lunar and Planetary Science Institute, Houston, TX, 1990, pp. 635–636.
- [31] R.C. Reedy, K. Nishiizumi, J.R. Arnold, Solar cosmic rays: fluxes and reaction cross sections, XX Lunar and Planet. Sci. Conf., Lunar and Planetary Science Institute, Houston, TX, 1990, pp. 890–891.
- [32] J. Beer, G.M. Raisbeck, F. Yiou, The variations of ^{10}Be and solar activity; in: C.P. Sonett et al. (Eds.), *The Sun in Time*, University of Arizona, Tucson, AZ, 1990, pp. 343–359.
- [33] G. Castagnoli, D. Lal, Solar modulation effects in terrestrial production of carbon-14, *Radiocarbon* 22 (1980) 133–158.
- [34] D. Lal, In-situ produced cosmogenic isotopes in terrestrial rocks, *Annu. Rev. Earth Planet. Sci.* 16 (1988) 355–388.
- [35] W.M. McElhinny, W.E. Senanayake, Variations in the geomagnetic dipole 1: the past 50,000 years, *J. Geomagn. Geoelectr.* 34 (1982) 39–51.
- [36] E. Tric, J.-P. Valet, P. Tuceolka, M. Paterne, L. Labeyrie, F. Guichard, L. Tauxe, M. Fontugne, Paleointensity of the geomagnetic field during the last 80,000 years, *J. Geophys. Res.* 97 (B6) (1992) 9337–9351.
- [37] E. Bard, Nuclide production by cosmic rays during the last ice age, *Science* 277 (1997) 532–533.
- [38] Y. Guyodo, J.-P. Valet, Relative variations in geomagnetic intensity from sedimentary records: the past 200,000 years, *Earth Planet. Sci. Lett.* 143 (1996) 23–36.
- [39] M. Frank, B. Schwarz, S. Baumann, P.W. Kubik, M. Suter, A. Mangini, A 200 kyr record of cosmogenic radionuclide production rate and geomagnetic field intensity from ^{10}Be in globally stacked deep-sea sediments, *Earth Planet. Sci. Lett.* 149 (1997) 121–129.